Physics of the Earth and Planetary Interiors, 8 (1974) 1–12
North-Holland Publishing Company, Amsterdam – Printed in The Netherlands

CONSTRAINTS ON TEMPERATURES BENEATH ICELAND FROM MAGNETOTELLURIC DATA *

JOHN F. HERMANCE and LARRY R. GRILLOT
Department of Geological Sciences, Brown University, Providence, R.I. (U.S.A.)

Accepted for publication April 4, 1973

The interpretation of magnetotelluric data from southwest Iceland provides three constraints on regional temperatures for the crust and upper mantle. First, it appears that temperature gradients from boreholes one or two kilometers deep (60–120°C/km) can be linearly extrapolated to the base of the crust. Second, the temperature at the crust–mantle interface (10–15 km) is in the range 1000 ± 200°C. Third, the temperature gradient in the upper mantle (15–100 km) is remarkably small and must be close to 1°C/km.

Although the absolute value of temperature is uncertain, a distinct difference emerges between the range of temperatures estimated from the magnetotelluric interpretation and the range of temperatures theoretically calculated from the conventional heat-flow equation. These differences, we feel, are a direct manifestation of the tectonic setting of Iceland.

1. Introduction

The following discussion attempts to place constraints on expected temperatures in the upper mantle beneath Iceland through the analysis of long-period magnetotelluric data. Iceland straddles the mid-ocean rift system in the North Atlantic and knowledge of temperatures in the upper mantle may help to understand physical processes beneath a strategic tectonic region.

The traditional method of estimating temperatures in the earth relies on solving the heat-flow equation, which involves assuming a plausible distribution of radioactive heat sources and the time-rate of change of temperature from some initial condition, the so-called thermal history of the earth (Jacobs and Allan, 1956; Clark and Ringwood, 1964; MacDonald, 1965; Lubimova, 1967; Ringwood, 1969). In Fig. 1 we have illustrated a number of such geotherms from the literature. Generally speaking oceanic geotherms have higher temperatures at a given depth than continental geotherms. An exception to this is Lubimova's continental geotherm (LC). The two oceanic geotherms (MO) of MacDonald (1965) show the effect of assuming different concentrations of radioactive heat sources in the model calculations; uranium concentrations of $5.5 \cdot 10^{-8}$ g/g and $3.3 \cdot 10^{-8}$ g/g, respectively. On the other hand, the difference between the Clark and Ringwood (1964) oceanic geotherm (CRO) and the oceanic geotherm (RO) of Ringwood et al. (1964) reflects different assumptions regarding the opacity of the upper mantle to radiative heat transfer.

Therefore, the rather broad range of temperatures permitted by these calculations (Fig. 1) appears to reflect uncertainties regarding both the distribution of heat sources within the earth as well as the actual thermal conductivity mechanism.

An alternative way to estimate temperatures inside the earth is to use electromagnetic data to determine electrical conductivity as a function of depth; then to convert these conductivities to temperature estimates by comparing them with laboratory measurements on

* This paper was presented at the I.A.G.A. Workshop on Electromagnetic Induction, held at the University of Edinburgh, 20th–27th September, 1972.

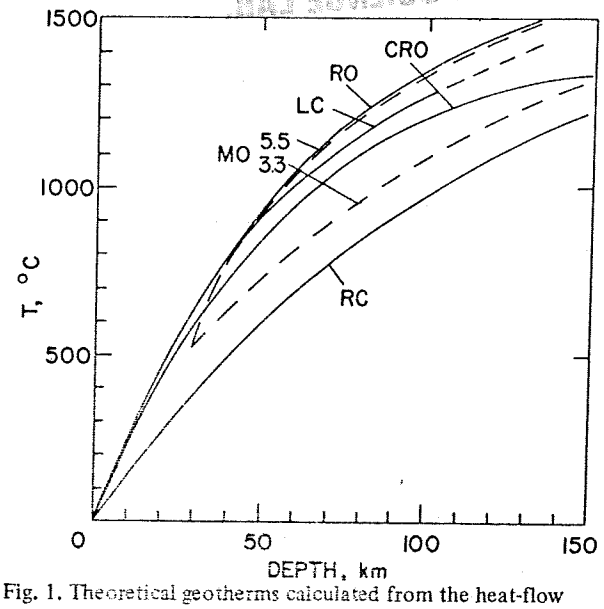

Fig. 1. Theoretical geotherms calculated from the heat-flow equation. The last letter in each label denotes oceanic (O) or continental (C) geotherms calculated by the following workers: CR, Clark and Ringwood (1964); M, MacDonald (1965); L, Lubimova (1967); R, Ringwood et al. (1964).

the conductivity of possible upper-mantle components as a function of temperature.

In the following discussion we use the latter technique to invert magnetotelluric data from Iceland to obtain constraints on temperature estimates for the upper mantle. Eventually we will return to the results in Fig. 1 by pointing out that although uncertainties exist both in temperatures theoretically estimated from the heat-flow equation, as well as temperatures estimated on the basis of magnetotelluric data, distinct differences nevertheless emerge between the range of temperatures obtained from the two methods. These differences, we feel, reflect the tectonic setting of Iceland.

2. The magnetotelluric data

The location of the field site at which data were obtained is shown in Fig. 2. The site is a few kilometers north of Lake Thingvallavatn in southwest Iceland, approximately 100 km from the intersection of the Mid-Atlantic Ridge with the western tip of the Reykjanes

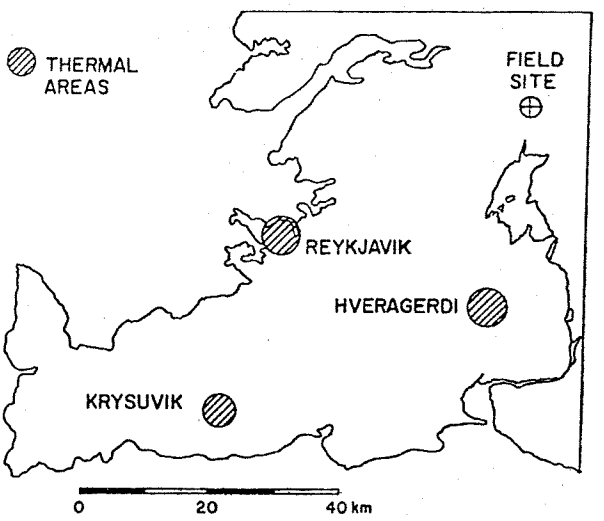

Fig. 2. Location of magnetotelluric field site in southwest Iceland.

Peninsula. This is the same site (THI) used by Hermance and Grillot (1970) for an earlier interpretation at intermediate periods.

For situations in which the electral conductivity changes in the vertical direction, orthogonal electric and magnetic field components can be used to determine an apparent resistivity as a function of period through the Cagniard (1953) relation:

$$\rho_a = 0.2\,T \left|\frac{E_x}{H_y}\right|^2 = 0.2\,T \left|\frac{E_y}{H_x}\right|^2 \qquad (1)$$

where ρ_a is the apparent resistivity in ohm-meters, T is the period in sec, E_x, E_y and H_x, H_y are the Fourier spectral amplitudes of the horizontal electric and magnetic field components in millivolts per kilometer and gammas, respectively, recorded along orthogonal measuring axes.

However, in the presence of lateral changes in the electrical properties of the earth, *each* electric field component couples to *both* magnetic field components through a relationship of the form:

$$E_x = Z_{xx}H_x + Z_{xy}H_y$$

$$E_y = Z_{yx}H_x + Z_{yy}H_y$$

where the matrix:

$$\begin{bmatrix} Z_{xx} & Z_{xy} \\ Z_{yx} & Z_{yy} \end{bmatrix}$$

is called the impedance tensor (Cantwell, 1960; Bostick and Smith, 1962). Clearly, this results in a more complicated relation for the apparent resistivity. On the other hand, if it should turn out, during the course of the analysis, that in fact the magnitudes of the diagonal tensor elements Z_{xx} and Z_{yy}, which couple parallel electric and magnetic field components, should be negligible compared to the magnitude of the off-diagonal elements Z_{xy} and Z_{yx}, which couple orthogonal electric and magnetic field components, and if the magnitudes of Z_{xy} and Z_{yx} are similar in value, then these observations are sufficient to suggest that the earth's conductivity is essentially a function of *depth* only, and if *lateral* inhomogeneities are indeed present, they have second-order effects on the behavior of the fields.

A recent review by Hermance (1973a) describes a number of methods devised by various workers to determine the complex tensor elements. In Fig. 3, tensor elements were estimated using the record-averaging technique of Sims et al. (1971) and the magnitudes of the diagonal (Z_{11}) and off-diagonal (Z_{12}) elements are compared as a function of rotation angle at a period of 50 sec. In Fig. 4, we compare tensor elements at 1000 sec calculated using the frequency-band averaging technique of Madden and Nelson (1964). These two figures support the earlier claim of Hermance and Grillot (1970) that at intermediate periods (50–1000 sec) magnetotelluric data from this site are relatively insensitive to lateral inhomogeneities. In other

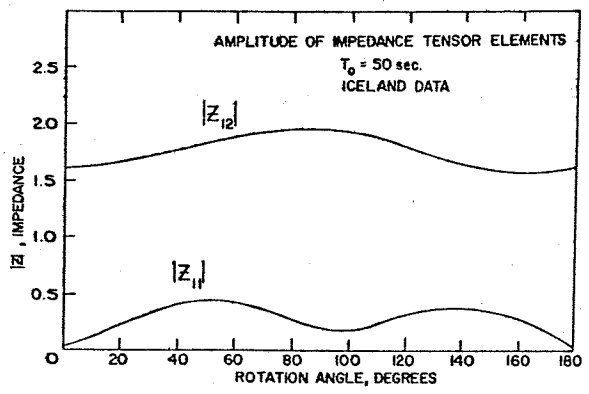

Fig. 3. Magnitudes of tensor elements at 50-sec period as a function of rotation angle. Z_{11} = diagonal element, Z_{12} = off-diagonal element.

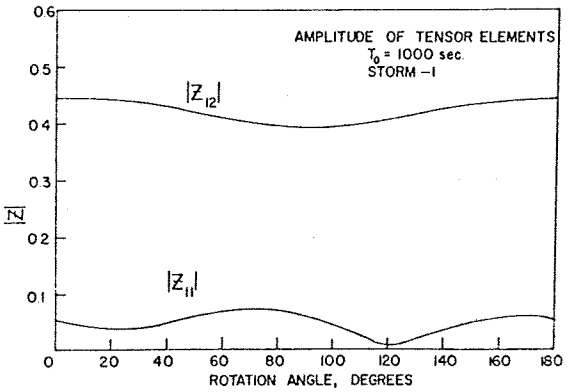

Fig. 4. Magnitudes of tensor elements at 1000-sec period as a function of rotation angle.

words, magnetotelluric fields are dominated by the *vertical* electrical structure rather than the *horizontal* electrical structure.

Maximum and minimum principal apparent resistivity values are plotted as a function of period in Fig. 5. The tensor elements themselves were calculated using an algorithm devised by Grillot (1973), and apparent resistivities were calculated from off-diagonal tensor elements rotated so as to minimize the diagonal elements (Bostick and Smith, 1962).

The analysis of the longest period data (2,000–16,000 sec) was performed using Fourier transient analysis of two magnetic substorms. Characteristically these phenomena display a strong polarization

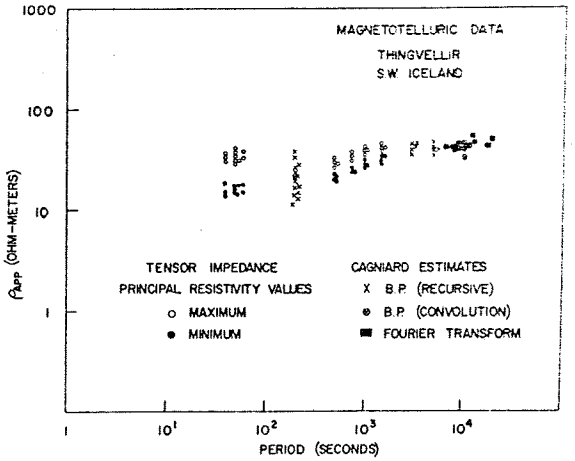

Fig. 5. Apparent resistivity data as a function of period. At periods where tensors could be calculated, maximum and minimum principal resistivity values are shown.

of magnetic variations close to the geomagnetic meridian; hence it was not possible to determine the tensor elements at very long periods. Instead we used eq. 1. For these particular calculations, the actual quantities substituted into eq. 1 were the amplitudes of the electric and magnetic field components projected onto the major axis of their respective polarization ellipse. A similar procedure was carried out with data band-pass filtered at 10^4 sec with good agreement between the two techniques as shown in Fig. 5.

Although apparent resistivities at long periods were essentially simple Cagniard (1953) estimates, we feel they are reliable for two reasons:

(1) The horizontal electric and magnetic polarization ellipses were orthogonal for two independent substorms. This is a necessary condition, even though it is not a sufficient condition, for the Cagniard equation to be valid.

(2) The diagonal elements of the tensor impedance are small at the longest period (2000 sec) for which independent field polarizations are available. This is indicated by the small differences between maximum and minimum apparent resistivity values at 1500 sec period in Fig. 5.

Extrapolating the range between maximum and minimum principal resistivities calculated at 2000-sec period to longer periods, we see in Fig. 5 that this range encompasses the uncertainty in our Cagniard estimates (40–50 Ωm). These observations suggest to us that if the impedance does indeed have a tensor quality at these long periods then the maximum and minimum principal resistivities probably fall close to the range 40–50 Ωm.

Since apparent resistivity data in Fig. 5 provide the basis of the following discussion, it is appropriate at this time to point out two features upon which our interpretation depends. The first is the inflection of the data between 100 and 1000 sec suggesting the transition to a more resistive medium at depth. The second is the rather constant value of apparent resistivity at periods longer than 1000 sec, which suggests a layer of uniform resistivity and great thickness at depth.

The next step in our discussion is to appraise quantitatively the range of models that generate the above two features.

3. Monte Carlo inversion of magnetotelluric data

In order to determine the range of one-dimensional resistivity models that generate apparent resistivities falling within the data envelope of Fig. 5, we have used a Monte-Carlo inversion technique as described by Greenfield and Turnbull (1970). The method essentially consists of representing the earth by a number of layers (N) having a fixed thickness, and specifying a number of discrete values of resistivity within each layer (M).

Models are then selected at random from a total of M^N possible cases. The magnetotelluric response is calculated for each model selected and tested against the field data, in our case the data envelope in Fig. 5. At the present time we have tested several tens of thousands of models against our data.

The best way of summarizing the results of testing such a large number of models is not obvious; a number of alternative ways present themselves. One useful parameter is the *frequency of occurrence* of resistivity values in each of the model layers that, upon inversion, successfully generate apparent resistivities falling within the range of the experimental data. This parameter, however, must be used with caution.

The details of our inversion procedure are given below. The procedure was divided into two phases. The first phase was a reconnaissance study to obtain a broad idea of models that would fit the field data. The second phase was a more restricted study in which the models were constrained to agree with recent seismic refraction studies by Palmason (1971).

3.1. Phase I: reconnaissance of possible models

In the first phase of our interpretation we investigated more closely our earlier suggestion (Hermance and Grillot, 1970) that the inflection of the data between 100 and 1000 sec period is caused by a resistivity increase across an interface 10–15 km deep. We have investigated both the range of resistivity contrasts across this interface and the sensitivity of the magnetotelluric data to the absolute depth of this interface.

Representing the earth's crust by three layers

TABLE I

Ranges of permissible models for Monte-Carlo inversion.
Phase I: reconnaissance of possible models

Layer no.	Resistivity range (Ωm)	Thickness (km)	Number of resistivity values in range
1	1200	0.7	1
2	10–200	2.3	6
3a*	1–33	7.	5
3b	1–33	12.	5
3c	1–33	17.	5
4	40–400	30.	5
5	20–400	60.	6
6	10–200	half-space	5

* Calculations were made for three thicknesses of Layer 3.

having resistivities within the ranges shown in Table I, the thickness of Layers 1 and 2 were fixed and separate inversions were performed for Layer 3 having three thicknesses: 7, 12, 17 km. In all cases Layer 4 was constrained to have a higher range of resistivities than Layer 3, so that by changing the thickness of Layer 3, the depth to the resistive interface was either at 10, 15 or 20 km. The thicknesses of Layers 4 and 5 were kept fixed, but since the thickness of Layer 3 increased, the true depths to the tops of Layers 4, 5 and 6 (the lower half-space) increased.

A surface layer (Layer 1) having a resistivity of 1200 Ωm and 0.7 km thick is required by active dipole–dipole measurements (Hermance, 1973b).

Fig. 6 summarizes the pattern of successful Monte-Carlo inversions. Layer 1 is constrained to a single resistivity and a single thickness as discussed above. Its parameters are represented by a single vertical line at 1200 Ωm, drawn from the surface to a depth of 0.7 km. The horizontal brackets represent the range of possible resistivities for each layer as given in Table I. The range of resistivities in Layer 2, for example, is 10–200 Ωm both in Table I and in Fig. 6.

The brackets, in Fig. 6, are drawn at the depth to the top of each layer represented.

To investigate the absolute depth of the resistive interface, Layer 3 was assigned three different thicknesses (models 1, 2 and 3) which place the resistive interface at a total depth of 10, 15 or 20 km. Therefore

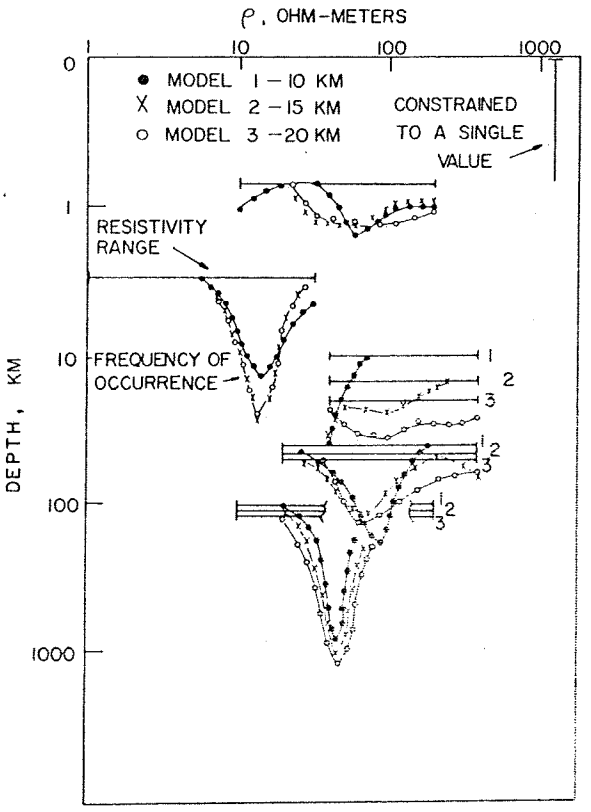

Fig. 6. Monte-Carlo inversion, Phase I. Models were run with three different depths (10, 15, 20 km) assigned to the resistive interface. The horizontal brackets show the range of permissible resistivities and are drawn at a depth corresponding to the top of the respective layers. A vertical line signifies that the resistivity throughout the layer is constrained to a single value. Curves show the frequency of occurrence of layer resistivities successfully fitting field data upon inversion.

the tops of all layers deeper than this (Layers 4, 5 and 6), are at three different depths as shown in Fig. 6.

The curves corresponding to each horizontal bracket are the frequency of occurrence of resistivity values in the layer directly beneath the bracket for models successfully fitting the field data. The black dots, crosses and open circles respectively correspond to total depths of 10, 15 and 20 km to the resistive interface.

The following pattern emerges from Phase I of our Monte-Carlo inversions:

(1) The experimental data are insensitive to the resistivity of Layer 2, whereas the resistivity of Layer 3 is reasonably well-defined.

(2) The absolute depth to the resistive interface is poorly defined, probably because of the relative breadth of the data envelope in Fig. 5 at periods of around 100 sec. However, for the interface at 10 or 15 km, resistivities near the low end of the permissible range have a higher frequency of occurrence.

(3) The resistivity at a depth of 100 km is well defined and appears to have a value in the range 40–50 Ωm.

(4) The frequencies of occurrence of resistivities in Layers 4, 5 and 6 suggest that actual resistivities may not vary by much more than a factor of two from 15 to 100 km depth.

3.2. Phase II: Resistive interface constrained to seismic interface (10 km)

The next phase of the Monte-Carlo inversion procedure was to invoke an earlier suggestion (Hermance and Grillot, 1970) that the resistive interface coincides with the crust–mantle seismic interface at 10 km as determined by Palmason (1971). Our purpose was to explore the range of possible resistivities in both the lower crust and upper mantle. The model parameters are given in Table II, and Fig. 7 summarizes the pattern of successful Monte-Carlo inversions. Layer 1 is constrained as in Phase I. The selection of successful models (Fig. 5) was insensitive to the resistivity of Layer 2 so its value was constrained to the mid-point of its range in Phase I. On the other hand, in Phase I, the successful models were very sensitive to the resistivity of the half-space below a depth of 100 km, and constraining its value to 45 Ωm is strictly required by the field data.

In summary the pattern of successful inversions in Fig. 7 suggests the following conclusions: (1) the true resistivity at the base of the crust appears to be in the range of 50–20 Ωm; (2) the true resistivity at the top of the mantle (10 km) appears to be in the range 40–100 Ωm; (3) resistivities in the upper mantle show surprisingly little variation from 10 km to 100 km and greater depth.

TABLE II

Ranges of permissible models for Monte-Carlo inversion. Phase II: resistive interface constrained to seismic interface (10 km)

Layer no.	Resistivity range (Ωm)	Thickness (km)	Number of resistivity values in range
1	1200	0.7	1
2	50	1.3	1
3	10–20	4.	5
4	1–20	4.	10
5	40–400	30.	10
6	20–400	60.	10
7	45	half-space	1

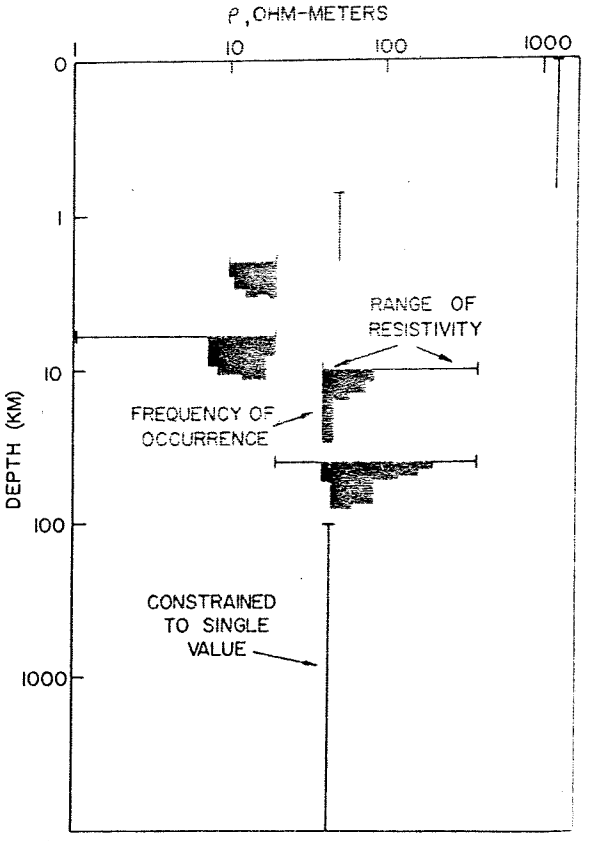

Fig. 7. Monte-Carlo inversion, Phase II. Models were run with the depth to the resistive interface constrained to a single value, 10 km. The histograms show the frequency of occurrence of layer resistivities successfully fitting field data upon inversion. Other conventions are the same as in Fig. 6.

Temperatures at the crust–mantle boundary

By relating the electrical interface at 10 km depth to the seismic crust–mantle boundary, we are provided with compositional control. Although there is a sharp gradient in composition from a basic crust to an ultrabasic upper mantle, a necessary condition is that at the interface, temperatures must be continuous. We now describe how this constraint is invoked to estimate temperatures at the crust–mantle boundary.

In Fig. 8 and 9, laboratory data are shown on the conductivity as a function of temperature for basalt and for ultrabasic materials, respectively, obtained by workers identified in the figure captions. Our approach has not been to specify a single-valued function of conductivity as a function of temperature, but to use the range of conductivities encompassing a number of measurements suggested by the area within the dashed lines on each figure. However, even these broad limits reflect a certain selection process.

In Fig. 8, we have excluded measurements on samples specifically identified as andesite basalt, feeling that this basalt type was not characteristic of ocean-crust composition.

Many more laboratory measurements on ultrabasic materials (olivene, peridotite) are cited in the literature, but few extend into the conductivity–temperature range of Fig. 9. For example, all of Hamilton's (1965) temperatures and conductivities are too low. Moreover, the only measurements of Duba (1972) that fall within the range of the figure are for a sample containing 26.4% fayalite which is a composition not compatible with most petrological models of the upper mantle. The data of Duba, however, are shown in Fig. 11, and are discussed presently.

Certain other measurements have been purposely excluded from the interpretation. Data on two samples of peridotite cited by Parkhomenko (1967) are not shown since they too lie outside the range of Fig. 9 and appear singularly anomalous. These samples displayed conductivities on the order of 10^{-2} mho/m at a temperature of 200°C.

We have also not used the measurements of Hughes (1955) on a gem-quality single crystal specimen of Red Sea peridotite. Although there seems to be some ques-

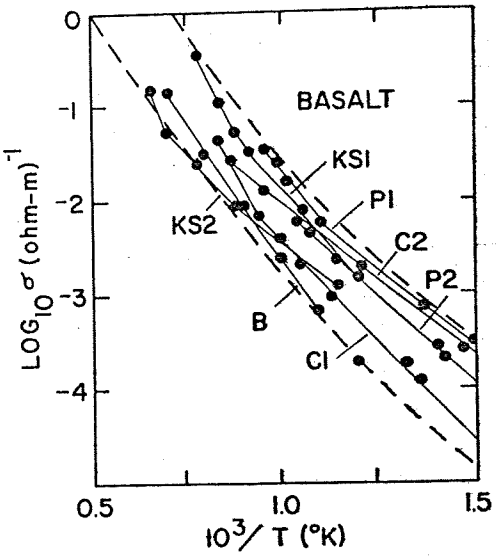

Fig. 8. Laboratory data on the electrical conductivity of basalt as a function of temperature. C, Coster (1948), 2 samples; P, Parkhomenko (1967), 2 samples; KS, Khitarov and Slutskiy. (1965), 2 samples; B, Bondarenko (1968), one set of data representing average characteristics of 200 specimens.

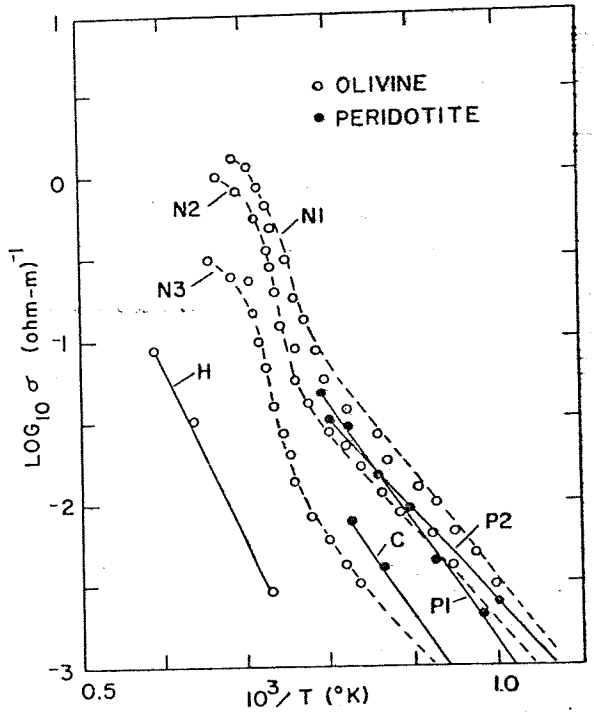

Fig. 9. Laboratory data on the electrical conductivity of ultrabasic materials as a function of temperature: N, Noritomi (1961), 3 samples of olivine; C, Coster (1948), 1 sample of peridotite; P, Parkhomenko (1967), 2 samples of peridotite; H, Hughes (1955), 1 sample of peridotite. The interpretation used the range of data between the outer dashed lines.

tion regarding the experimental technique of these measurements (Hamilton, 1965; Duba, 1972), our reason for excluding these data is that measurements of such pure samples, even if useful for studying conductivity mechanisms in simple magnesium silicates, may not be particularly relevant to actual bulk characteristics of the upper mantle itself. Conceivably, mantle materials should have a greater concentration of impurities, hence a greater conductivity at the temperatures discussed here, than pure magnesium silicate.

The area within the dashed lines of Fig. 8, then, is characteristic of the conductivity–temperature behavior of deep crustal materials, whereas the area within the dashed lines of Fig. 9 is thought to be characteristic of upper-mantle materials.

The next step is to project the range of in-situ resistivities estimated from the magnetotelluric interpretation onto the respective data envelopes of Fig. 8 and 9. This is summarized schematically in Fig. 10 where we show the temperatures obtained by projecting the upper and lower limits of resistivity above the interface (5–20 Ωm) onto the data envelope of basalt in Fig. 8. This temperature range is then compared with the temperatures obtained by projecting the upper and lower limits of resistivity below the interface (40–100 Ωm) onto the data envelope of ultrabasic materials in Fig. 9. We also show for comparison in Fig. 10, the temperature range estimated by projecting an assumed value of 10 Ωm for the lower crust onto the laboratory data (not shown) of Khitarov et al. (1970) for three types of tholeiitic basalt (Ol: olivene; Qtz: quartz; Al: aluminum).

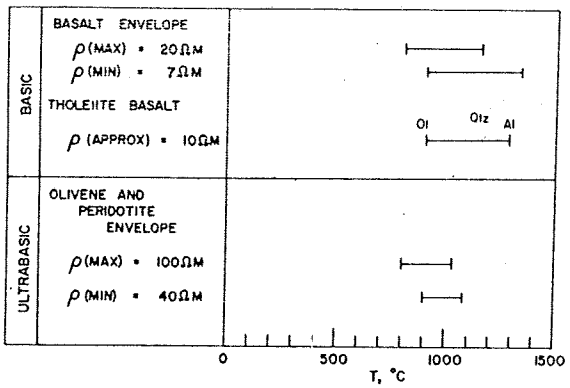

Fig. 10. Range of temperatures at crust–mantle boundary inferred from magnetotelluric data. The maximum and minimum values of resistivity for the basic crust and ultrabasic mantle are based on the Monte-Carlo inversions (Fig. 6 and 7). Each of these resistivities was projected onto the envelope of the appropriate laboratory data (Fig. 8 or Fig. 9) to obtain the temperature range shown.

We observe from Fig. 10 that the range of temperature estimates above the interface overlaps the range of temperature estimates below the interface. Therefore, our interpretation agrees with the physical constraint that temperatures must be continuous across the interface, allowing us to estimate that temperatures at a depth of 10 km are within the range 1000 ±200°C.

5. Electrical effects of water in the crust

The laboratory specimens discussed in the last section were generally oven-dried using conventional techniques to drive out interstitial water. An important question arises: Suppose water was present, what could its electrical effects be? The question becomes pressing, since we know for surface rocks that the electrical properties are dominated by the effects of conduction along pores and cracks containing electrolytic fluids (Keller and Frischknecht, 1966). If this is the case for surface rocks, could not the effects of water, if present, completely dominate the conduction mechanism in the deep crust, thus making the interpretation in the last section meaningless?

The effects of electrolytic fluids in the crust beneath Iceland are investigated in a recent paper by Hermance (1973b). The question is far from being resolved, but calculations using simple models suggest the following conclusions: (1) the suppression of resistivity at shallow depth is caused by regional hydro-thermal activity; (2) appreciable effects from water are obtained from depths 8–10 km; (3) below 10 km the effects from conduction along electrolytic paths are dominated by conduction in the solid rock itself.

The third conclusion does not say that water is absent at depths of 10 km, but rather that ionic association in the electrolyte is increasing to such an extent at the high temperatures anticipated, that the electrical effects of the pore fluid are minimized.

We therefore conclude that the effects of water, even if it was present, would not significantly alter the interpretation of section 4.

6. Thermal gradients in the upper mantle

6.1. Comments on laboratory conductivity data

Systematic investigations in the recent literature (Hamilton, 1965; Shankland, 1969; Duba, 1972) have underlined a number of problems in laboratory measurements on electrical conductivity as a function of temperature and pressure. We only mention several of these problems by way of illustration without discussing them in detail.

First, we do not know the precise composition of the upper mantle, and both Hamilton (1965) and Duba (1972) have pointed out that, even in a simple forsterite–fayalite ($Mg_2SiO_4-Fe_2SiO_4$) solid solution series, in going from fayalite-poor compositions to fayalite-rich compositions, the absolute conductivity may change by several orders of magnitude, as shown in Fig. 11. Moreover, the oxidation state of specimens having basically the same composition seems to alter significantly the conductivity at a given temperature (Duba, 1972).

Another problem appears to be uncertainty in the pressure-coefficient of conductivity. Although the pressure-effect on total conductivity appears to be relatively small, the sign of the pressure coefficient is uncertain, differing among various workers (Hamilton, 1965; Coster, 1948; Hughes, 1955). In a carefully performed suite of measurements, Duba (1972) has pointed out inconsistencies among his various samples as well. For example, the pressure derivative of his 8.2 mol% fayalite was opposite to all other compositions. He suggests that this "pressure-effect" could be due to experimental procedure and is not real, and urges caution in the interpretation of pressure-coefficients from other workers.

Clearly, the pressure coefficient would be a valuable parameter to incorporate into the later part of our discussion, although it seems from the current literature we must be content with assessing the limits of its effect, rather than using it quantitatively. In short, we might expect pressure-effects to change the conductivity by as much as a factor of two over 100 km depth, although it is uncertain whether the effect would be an increase or decrease.

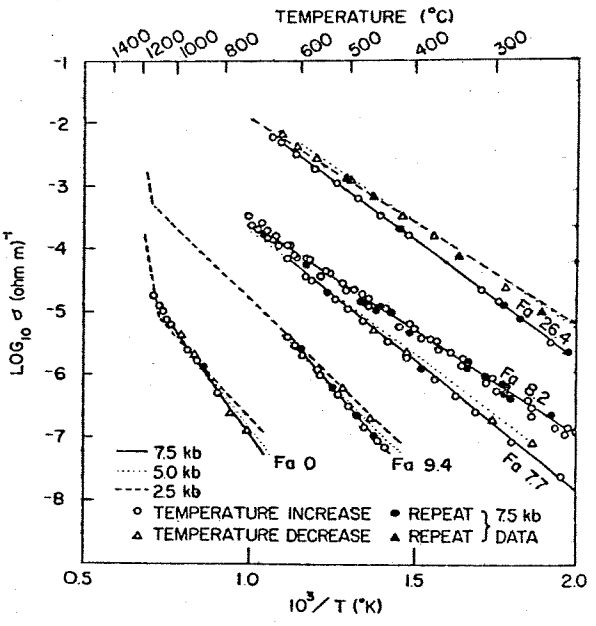

Fig. 11. Laboratory data after Duba (1972) on the temperature dependence of the electrical conductivity of olivene for various concentrations of fayalite (in mole-percent) for the solid solution series: $Mg_2SiO_4-Fe_2SiO_4$. These data illustrate that although composition drastically changes the absolute conductivity at any temperature, the change of the logarithm of conductivity with temperature is similar for a range of compositions.

6.2. Temperature gradients as opposed to absolute temperatures

Data from Duba (1972) on electrical conductivity versus temperature are plotted in Fig. 11 for various samples in the forsterite–fayalite solid solution series. Numbers for each curve correspond to the mole-percent of fayalite. The first impression one obtains from this figure is the broad range of conductivity for various compositions, at the same temperature. This reflects the point made previously of the difficulty in assessing absolute temperatures at depth because of uncertainty in composition.

On the other hand, another impression one obtains is the tendency for these curves to be parallel. This implies that although for various compositions absolute conductivities vary enormously, the change in conductivity (or the logarithm of conductivity, to be

precise) with temperature is similar for many possible upper-mantle materials. Since the slope of these lines is simply the activation energy, this implies that the activation energy is similar for many of these materials, which was pointed out by Hamilton (1965). The point is that the *change* of temperature with changing conductivity can be estimated more readily than the *absolute* value of temperature from the absolute value of conductivity.

One is led, therefore, to the idea of estimating a temperature gradient in the upper mantle, rather than absolute temperatures. We obtain this gradient in the following way.

By assuming the upper mantle is more or less homogeneous, it is plausible that the temperature dependence of resistivity over a restricted range can be approximated by the conventional relation:

$$\rho = ce^{E/kT} \tag{2}$$

where ρ is the resistivity, c is a constant, E is the activation energy, k is Boltzmann's constant, and T is the absolute temperature in °Kelvin.

The difference between the natural logarithm of the resistivity at depth 1 and depth 2 is related to the temperature at the same depths by:

$$\ln\rho_1 - \ln\rho_2 = \frac{E}{k}\left(\frac{1}{T_1} - \frac{1}{T_2}\right) \tag{3}$$

Upon substituting:

$$T_2 = T_1 + G_T z \tag{4}$$

where z is the difference between the two depths and G_T is the average geothermal gradient over the same range, and expanding eq. 3 as a binomial series, we obtain an expression for the average geothermal gradient:

$$G_T = \frac{kT^2}{Ez} \ln\frac{\rho_1}{\rho_2} \tag{5}$$

Assuming that the resistivity changes by a factor of 2 from a depth of 15–100 km, and that at 15 km, the temperature is 1000°C (1273°K), and assuming an activation energy of 1.3 eV, the parameters in eq. 5 become $E = 1.3$ eV, $T_1 = 1273$°K, $z = 85$ km, $\rho_1/\rho_2 = 2$, leading to an average geothermal gradient of:

$$G_T = 1\text{°C/km} \tag{6}$$

Because of uncertainties in the activation energy, the change of resistivity with depth and the pressure coefficient of total conductivity, this estimate is probably uncertain by a factor of two. Nevertheless geothermal gradients in the upper mantle appear to be significantly smaller than geothermal gradients in the cru

7. Constraints on Sub-Icelandic temperatures

The previous discussion is summarized in Fig. 12 to provide a system of constraints on temperature estimates beneath Iceland.

Surface geothermal gradients in boreholes 1 or 2 km deep, away from hydrothermal zones, lie within the range 60–120°C/km (Palmason, 1967). Because of the low heat productivity of basic rocks, it seems reasonable that these temperature gradients can be linearly extrapolated to the base of the crust. This hypothesis is supported by the magnetotelluric inte-

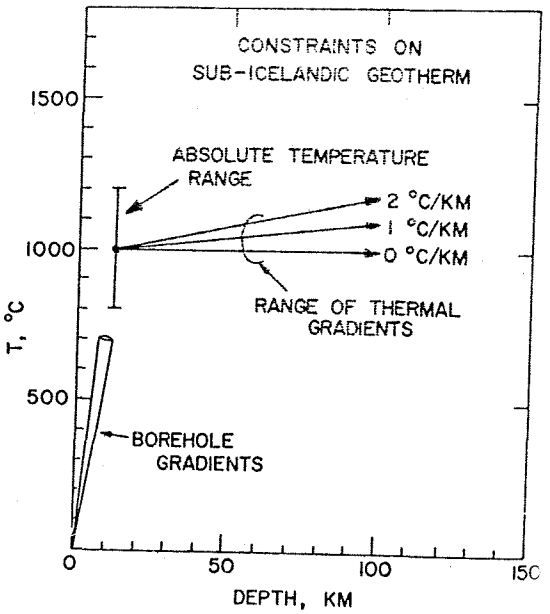

Fig. 12. Constraints on the Sub-Icelandic geotherm. Thermal gradients in boreholes lie within the range 60–120°C; absolute temperatures at the crust–mantle boundary fall within the range 1000 ± 200°C; and thermal gradients in the upper mantle are close to 1°C/km.

pretation discussed previously, which was that resistivities at the crust–mantle interface (10–15 km), suggest an absolute temperature range of 1000±200°C.

From the base of the crust to 100 km, the temperature gradient appears to be close to 1°C/km, but this is uncertain by a factor of two.

These constraints are integrated in Fig. 13 to estimate the range of temperatures beneath Iceland. The range of temperatures is slightly reduced from the maximum limits placed by a strictly magnetotelluric interpretation (Fig. 12), since other evidence is available. We have argued earlier that the upper mantle is partially-melted from the observation that P-wave velocities are reduced to 7.2 km/sec. The maximum temperature at the base of the crust then is 1100–1200°C based on the temperature of lava erupted at the surface. On the other hand, the melting-point temperature, even in the presence of significant amounts of water (Ringwood, 1969), cannot be much less than a supposed minimum of 900°C.

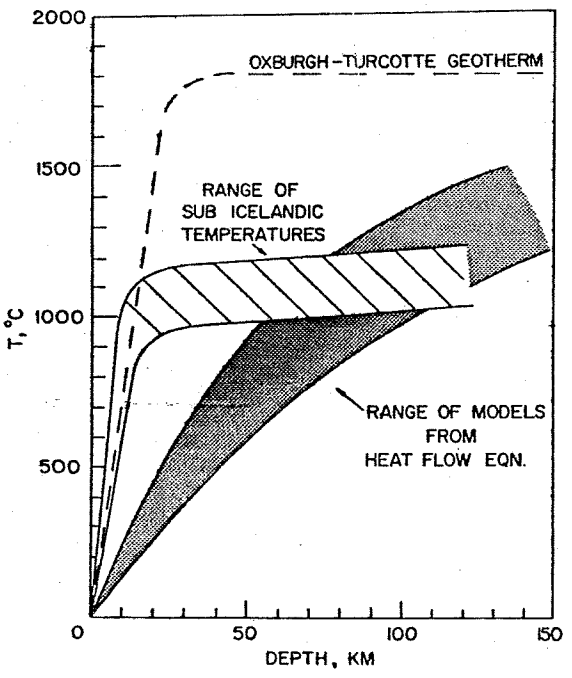

Fig. 13. Range of Sub-Icelandic temperatures inferred from magnetotelluric data compared with the range of temperatures calculated from the heat-flow equation. Also shown are temperatures theoretically calculated by Oxburgh and Turcotte (1968) for a primitive convection model.

Also shown in Fig. 13 is the range of theoretical calculations based on the heat-flow equation discussed in section 1, as well as the results of a calculation made by Oxburgh and Turcotte (1968) for a convecting upper mantle. It appears that upper-mantle temperatures are overestimated by the model of Oxburgh and Turcotte (1968), whereas conventional heat-flow models underestimate temperatures beneath Iceland to depths of 100 km.

Despite uncertainties in temperatures estimated from the magnetotelluric data, as well as uncertainties in temperatures theoretically calculated from the heat-flow equation, a significant difference between the two is apparent. In particular, thermal gradients in the upper mantle are two orders of magnitude less than thermal gradients in the crust. We feel that this difference is a direct manifestation of the dominant tectonic processes beneath Iceland which are not accounted for in the heat flow models discussed above. If, for example, temperatures in the crust and upper mantle are dominated by a vertical heat with flux negligible divergence, then the observation that temperature gradients are two orders of magnitude smaller in the upper mantle than in the crust requires that the thermal conductivity in the upper mantle be two orders of magnitude greater. Such an efficient transfer of heat may imply the bulk transport of material, perhaps either by the segregation of a partial melt phase or by flow of the mantle itself, or by a combination of both effects.

Acknowledgements

We would like to acknowledge the assistance and encouragement provided by Gudmundur Palmason and Sveinbjorn Bjornsson of the National Energy Authority of Iceland, as well as the many stimulating discussions with Paul Hess, of our department. Roy Greenfield of Pennsylvania State University supplied the Monte-Carlo inversion program.

Support for much of the research was provided by

N.S.F. Grants GA-11850, GA-30101, GA-26142 and GA-37092.

References

Bondarenko, A.T., 1968. Dokl. Akad. Nauk SSSR, 178: 20.

Bostick, F.X. and Smith, H.W., 1962. Proc.Inst. Radio Eng., 50: 2339.

Cagniard, L., 1953. Geophysics, 18: 605.

Cantwell, T., 1960. Detection and Analysis of Low-Frequency Magnetotelluric Signals. Thesis, Geophys. Lab. M.I.T., Cambridge, Mass., p. 171.

Clark, S.P. Jr. and Ringwood, A.E., 1964. Rev. Geophys., 2: 35.

Coster, H.P., 1948. Mon. Not. R. Astron. Soc., Geophys. Suppl. 5: 193.

Duba, A., 1972. J. Geophys. Res., 77: 2483.

Greenfield, R.J. and Turnbull, L.S., Jr. 1970. EOS, Trans. AGU, 51: 426.

Grillot, L.R., 1973. Regional Electrical Structure beneath Iceland as determined from Magnetotelluric Data. Thesis, Brown Univ., Providence, R.I., 80 pp.

Hamilton, R.M., 1965. J. Geophys. Res., 70: 5679.

Hermance, J.F., 1973a. Phys. Earth Planet. Inter., 7: 349.

Hermance, J.F., 1973b. Geophysics, 38: 3.

Hermance, J.F. and Grillot, L.R., 1970. J. Geophys. Res., 75: 6582.

Hughes, H., 1955. J. Geophys. Res., 60: 187.

Jacobs, J.A. and Allan, D.W., 1956. Nature, 177: 155.

Keller, G.V. and Frischknecht, F.C., 1966. Electrical Methods in Geophysical Prospecting. Pergamon Press, New York, N.Y., p. 519.

Khitarov, N.I. and Slutskiy, A.B., 1965. Geochem. Int., 2: 1034.

Khitarov, N.I., Slutskiy, A.B. and Pugin, V.A., 1970. Phys. Earth Planet. Inter. 3:334.

Lubimova, E.A., 1967. In: T.F. Gaskell (Editor). The Earth's Mantle. Academic Press, New York, N.Y., p. 231.

MacDonald, G.J.F., 1965. In; W.H.K.Lee (Editor), Terrestrial Heat Flow–Geophys. Monogr. 8. Am. Geophys. Union, Washington, D.C., p.191.

Madden, T. and Nelson, P., 1964. A Defense of Cagniard's Magnetotelluric Method. Project NR-371-401. Geophysics Laboratory, M.I.T., 41 pp.

Noritomi, K., 1961. J. Mining Coll. Akita Univ., Ser. A, 1: 27.

Oxburgh, E.R. and Turcotte, D.L., 1968. J. Geophys. Res., 73: 2643.

Palmason, G., 1967. In: S. Bjornsson (Editor), Iceland and Mid-Ocean Ridges. Soc. Sci. Islandica, Rit '38', p. 128.

Palmason, G., 1971. Crustal Structure of Iceland from Explosion Seismology. Visindafelag Islendinga, Reykjavik, p. 187.

Parkhomenko, E.I., 1967. Electrical Properties of Rocks. Plenum, New York, N.Y., p.314.

Ringwood, A.E., 1969. In: P.J. Hart (Editor), The Earth's Crust and Upper Mantle.–Geophys. Monogr. 13. Am. Geophys. Union, Washington, D.C. p.1.

Ringwood, A.E., MacGregor, I.D. and Boyd, F.R., 1964. Carnegie Inst. Wash. Yearbook, 63: 147.

Sims, W.E., Bostick, Jr F.X., and Smith, H.E., 1971. Geophysics, 36: 938.

Shankland, T.J., 1969. In: S.K. Runcorn (Editor), Application of Modern Physics to Earth and Planetary Sciences. Wiley, London, p. 175.